Water Resources Research

RESEARCH ARTICLE
10.1029/2022WR033454

Aridification of Colorado River Basin's Snowpack Regions Has Driven Water Losses Despite Ameliorating Effects of Vegetation

Benjamin Bass[1], Naomi Goldenson[1], Stefan Rahimi[1], and Alex Hall[1]

[1]Department of Atmospheric and Oceanic Sciences, University of California, Los Angeles, CA, USA

Key Points:

- A 10.3% reduction in Colorado Basin's present-day natural flow exists due to anthropogenic warming despite vegetation response to CO_2
- Anthropogenic warming reduced Colorado Basin's natural flow by roughly the storage of Lake Mead during the ongoing megadrought (2000–2021)
- Greater aridification in snowpack regions is causing water losses to occur roughly twice as fast compared to non-snowpack regions

Supporting Information:

Supporting Information may be found in the online version of this article.

Correspondence to:

B. Bass,
benb0228@g.ucla.edu

Citation:

Bass, B., Goldenson, N., Rahimi, S., & Hall, A. (2023). Aridification of Colorado River Basin's snowpack regions has driven water losses despite ameliorating effects of vegetation. *Water Resources Research*, *59*, e2022WR033454. https://doi.org/10.1029/2022WR033454

Received 12 AUG 2022
Accepted 23 MAY 2023

Author Contributions:

Conceptualization: Benjamin Bass, Naomi Goldenson
Data curation: Stefan Rahimi
Formal analysis: Benjamin Bass
Investigation: Benjamin Bass
Methodology: Benjamin Bass
Resources: Benjamin Bass, Stefan Rahimi, Alex Hall
Supervision: Naomi Goldenson, Alex Hall
Writing – original draft: Benjamin Bass
Writing – review & editing: Naomi Goldenson, Stefan Rahimi, Alex Hall

Abstract The Colorado River Basin is an important natural resource for the semi-arid southwestern United States (US), where it provides water to more than 40 million people. While nearly 1.5°C of anthropogenic warming has occurred across this region from the 1880s to 2021, climate models show little agreement in the precipitation change during the same historical period, with no trend in the mean of the latest (sixth) generation of Global Climate Models. As such, here we focus on how the CO_2 increase and associated anthropogenic warming over the historical period has impacted runoff across the Colorado Basin. We find that the Colorado Basin's runoff over the historical period has decreased by 8.1% per degree Celsius of warming (°C^{-1}). However, the magnitude of this sensitivity is reduced to 6.8% °C^{-1} when considering vegetation response to historical CO_2. For present-day conditions, this translates to runoff reductions of 10.3% due to anthropogenic increases in both temperature and CO_2 since 1880. We demonstrate that Colorado Basin's natural flow has been decreased by roughly the storage of Lake Mead during the 2000–2021 megadrought due to this long term anthropogenic influence, suggesting the basin's first shortage in 2021 would likely not have occurred without anthropogenic warming. We further show warming has led to disproportionate aridification in snowpack regions, causing runoff to decline at double the rate relative to non-snowpack regions. Thus, despite only making up ~30% of the basin's drainage area, 86% of runoff decreases in the Colorado Basin is driven by water loss in snowpack regions.

Plain Language Summary The Colorado River Basin provides a crucial source of water for an expansive water-limited region covering the southwestern US and its major cities. Several studies have demonstrated that this basin has experienced substantial reductions in water availability due to warming. Here, we quantify how reductions in water availability have varied from 1954 to 2021 across this basin due to human-driven warming that has occurred since 1880. As a part of this analysis, we include how the vegetation response to historical increases in CO_2 has impacted water losses. We find that the basin has roughly 10% less water available under present-day conditions due to warming since the 1880s. The majority of water loss has occurred due to a heightened sensitivity to warming in the basin's regions associated with snowpack, compared to regions without snowpack. We also demonstrate that without this warming, the Colorado Basin would have had significantly larger amounts of water available, equal to the size of Lake Mead, over the duration of the 2000–2021 megadrought.

1. Introduction

The Colorado River Basin provides agricultural and municipal water for 40 million people, including every major city in the southwestern United States (US), both within (e.g., Phoenix, Las Vegas) and outside of the basin (e.g., Los Angeles, Denver, Albuquerque). Given the importance of this freshwater resource and the severity of the ongoing 21st-century drought (Williams et al., 2020, 2022), several recent studies have evaluated the sensitivity of the Colorado Basin's runoff or water availability in terms of the runoff change per temperature change (% °C^{-1}) (e.g., P. C. D. Milly & Dunne, 2020; Udall & Overpeck, 2017; Xiao et al., 2018). Previous studies have mostly focused on determining the sensitivity of the basin's runoff (% °C^{-1}), with estimates ranging from −2 to −12% °C^{-1} (Hoerling et al., 2019; McCabe & Wolock, 2007; P. C. D. Milly & Dunne, 2020; L. L. Nash & Gleick, 1991; Vano et al., 2012; Xiao et al., 2018). In general, previous studies evaluating runoff sensitivity use hydrologic models forced by perturbed present-day temperatures. Most commonly, the delta method is used, which evaluates the change in runoff during a particular time period when a 1°C warming is imposed (McCabe & Wolock, 2007; P. C. D. Milly & Dunne, 2020; L. L. Nash & Gleick, 1991; Vano et al., 2012). These studies have

advanced our understanding of runoff's sensitivity in the Colorado Basin; however, they leave open the question of how runoff has responded over time due to temporally varying rates of warming, including seasonal variations. Also, while such studies have highlighted the average runoff sensitivity (% $°C^{-1}$) for a given event or time-period, the runoff efficiency may vary between dry and wet years and may be more sensitive during drought conditions (Lehner et al., 2017).

To account for these heterogeneities, Xiao et al. (2018) performed historical hydrologic simulations over the Colorado Basin with the linear warming trend removed. While this allowed for an analysis of the impact of warming on drought events of interest, anthropogenic signals can be masked by natural variability, and anthropogenic signals can vary in time. For example, warming rates were generally slower from the 1880s–1940s, followed by a cooling trend from the 1940s–1970s driven by anthropogenic aerosols (Schwartz & Andreae, 1996; Wilcox et al., 2013), and in the past few decades warming has accelerated (Gillett et al., 2021). Here, we are interested in how the Colorado Basin has responded to time-varying anthropogenic warming over recent decades. This is achieved by using several Global Climate Models (GCMs) and their multiple realizations, which, when averaged, represent the anthropogenically forced component of the temperature change. We can then remove this component from the historical record to isolate natural variability in historical temperature. In our study, runoff's sensitivity (% $°C^{-1}$) in California's Sierra Nevada and the Columbia River Basin are briefly included for comparison to the Colorado Basin owing to their societal importance for water supply and dense observational streamflow allowing for more reliable assessments. However, we focus on the Colorado Basin given its heightened sensitivity (% $°C^{-1}$) compared to these other major western US riverine basins.

Another important and relatively unexplored area of uncertainty involves how the vegetation response to CO_2 may modulate the runoff sensitivity (% $°C^{-1}$). Several previous studies were unable to represent the vegetation response to CO_2 due to limitations in the hydrologic model employed (e.g., Vano et al., 2012; Xiao et al., 2018). As a result, such studies may have under- or over-estimated the sensitivity of runoff (% $°C^{-1}$) (X.-Y. Zhang et al., 2022). This is because as CO_2 increases there is a trade-off between decreasing transpiration due to stomatal closure (Piao et al., 2020; Zhu et al., 2017) and increasing transpiration due to greening or increases in leaf area index (LAI) (Fensholt et al., 2012; Zeng et al., 2018; Zhu et al., 2017). As suggested by X.-Y. Zhang et al., 2022, greening and stomatal closure should both be considered rather than ignoring the impact of both of these processes (e.g., Vano et al., 2012; Xiao et al., 2018) or only representing one of them (e.g., Mankin et al., 2019; P. C. Milly & Dunne, 2016; Yang et al., 2019). For our hydrologic simulations, we use the Noah Multiparameterization (Noah-MP) land surface model (LSM) with dynamic vegetation and transient CO_2 based on historically observed conditions. By doing so we can estimate the degree to which vegetation-CO_2 feedbacks may have impacted runoff sensitivity in the Colorado Basin during the historical period.

Of particular interest is the degree to which anthropogenic warming and CO_2 changes have influenced water availability during the ongoing megadrought from 2000 to 2021 and the more recent short-duration, high-intensity 2020–2021 drought. The megadrought (2000–2021) includes the driest 22-year precipitation across the western US during the observational historical record (Williams et al., 2022). During this prolonged drought, the 2020–2021 water years (WYs) also include the driest 20-month period of precipitation since 1895 (Mankin et al., 2021), and the lowest 2-years of natural flow from the Upper Colorado Basin since at least 1906 (Williams et al., 2022). While the precipitation deficit during 2000–2021 is primarily driven by natural variability (Mankin et al., 2021), long term anthropogenic warming has contributed to the exceptional warmth that also characterized this drought (Mankin et al., 2021). This anthropogenic warming has impacted variables commonly used to characterize drought, that depend on precipitation and temperature conditions, such as snowpack (Mote et al., 2018), soil moisture (Williams et al., 2022) and vapor pressure deficit (Mankin et al., 2021). Since the 2000–2021 megadrought led to the first-ever tier one shortage declared by the Bureau of Reclamation in the Lower Colorado Basin on August 2021 (AWWA, 2021; Bureau of Reclamation, 2022; Stern & Sheikh, 2022), we seek to answer how anthropogenic warming impacted streamflow during this megadrought and the shorter, high-intensity 2020–2021 drought, which pushed the Colorado Basin into its first tier one shortage.

In this study, we also seek to quantify the sensitivity of runoff (% $°C^{-1}$) for regions associated with snowpack versus those without snowpack, to enhance our understanding of the factors shaping the runoff sensitivity. Xiao et al. (2018) highlighted that larger runoff losses occur in basins associated with snowpack, while P. C. D. Milly and Dunne (2020) suggested warming-driven snowpack losses in the Colorado Basin are associated with higher evaporative losses; however, the runoff sensitivity (% $°C^{-1}$) of such regions has not been addressed. Such analysis

is important because snowpack-driven catchments within the Colorado Basin contribute roughly two thirds of the basin's total runoff while only making up roughly one third of its drainage area.

In summary, our objectives are to (a) evaluate how historical warming and the vegetation response to increases in CO_2 have impacted runoff across the Colorado Basin from 1954 to 2021, (b) provide detailed analysis for the prolonged drought (2000–2021) and the recent 2020–2021 drought, and (c) quantify the runoff sensitivity (% $°C^{-1}$) in snowpack versus non-snowpack regions. We focus our analysis on the warming component of anthropogenic climate change rather than any possible anthropogenic changes in precipitation. Anthropogenic changes in historical precipitation across the Colorado Basin are highly uncertain and characterized by neutral changes based on simulations from the latest phase of the Coupled Model Intercomparison Project (CMIP6) (IPCC AR6, 2021; Mankin et al., 2021).

2. Methodology

2.1. Forcing Dataset and Land Surface (Hydrologic) Model

In this study, we use Noah-MP given its capability to represent dynamic vegetation and vegetation response to transient CO_2 (Niu et al., 2011). As a forcing dataset, we use the European Centre for Medium-Range Weather Forecasts fifth Reanalysis (ERA5) dynamically downscaled with the Weather Research Forecasting climate model (WRF) (Rahimi et al., 2022). ERA5 was downscaled with WRF (henceforth, referred to as ERA5-WRF) to 9 km resolution across the western US from September 1951 to August 2021. Throughout the manuscript, we refer to the year alone, which, for example, represents September 1988 to August 1989 for the year 1989. Thorough testing was performed with WRF to reduce precipitation and snowpack biases in downscaling ERA5. As outlined in Rahimi et al. (2022), key parameterizations used in dynamical downscaling of ERA5, included P3 microphysics (Morrison & Milbrandt, 2015), the Tiedtke cumulus scheme (Tiedtke, 1989; C. Zhang et al., 2011), the Yonsei University planetary boundary layer scheme (Hong et al., 2006), and the longwave and shortwave broadband radiative transfer code for general circulation model applications (RRTMG) (Iacono et al., 2008).

Our Noah-MP LSM, which is driven by WRF-Hydro version 5.1.1 (Gochis et al., 2020), has the same grid spacing (9 km) and domain (the western US) as the ERA5-WRF forcing data. To obtain streamflow, gridded runoff from Noah-MP was aggregated across a given watershed and weighted by the fraction of a grid cell's area within a basin. A 3-hr time-step was used to run Noah-MP, and simulations were performed from 1951 to 2021 with the first 3-year used as the spin-up time-period. Major riverine basins entirely captured within our domain, include the Colorado River Basin, Columbia River Basin, and California's Sierra Nevada (Figure 1). However, while our simulated domain covers the western US (Figure 1a), this study focuses on the Colorado Basin given its relatively high sensitivity (% $°C^{-1}$) (later demonstrated). Note, we exclude Gila Basin which is located in the southeastern portion of the Colorado Basin. The Gila Basin is excluded since it is the only ungauged portion of the Colorado Basin, in recent years it has mostly been nearly dry, and since 1964 it has been excluded as a part of the Colorado River Compact (Xiao et al., 2018). The model's land use or vegetation were aggregated from USGS 30 arc-second 24-category land use and vegetation data (USGS, 2018), and the soil type was similarly aggregated from 30 arc-second hybrid State Soil Geographic Database soil texture data sets (NCAR, 2022). Initial (pre-calibration) land surface parameters in Noah-MP are based on these datasets via the use of Noah-MP look-up tables relating soil and vegetation types to their expected parameters. Due to space limitations, we provide an outline of the calibration procedure that was employed to improve the representation of Noah-MP's streamflow in Supporting Information S1 (Text S1 in Supporting Information S1).

Notably, after calibration, we modified the static vegetation parameterization in Noah-MP to represent dynamic vegetation. Noah-MP uses a simple but efficient dynamic vegetation model (Dickinson et al., 1998) that represents photosynthesis, carbon allocation, respiration, turnover, and leaf death due to temperature and water stresses (Niu et al., 2011). When using dynamic vegetation in Noah-MP, the Ball-Berry parameterization for stomatal resistance must be selected, where leaf-level stomatal conductance is controlled by non-biological factors such as atmospheric humidity and CO_2 concentration (Ball et al., 1987). As described in greater detail in Niu et al., 2011, when CO_2 increases, the dynamic vegetation model represents the stomatal closure effect on transpiration and a greening effect due to carbon assimilation that leads to increased transpiration. To represent historical changes in the concentration of CO_2, we obtained data from Mauna Loa Global Monitoring Laboratory, which began measurements in 1958 (Keeling et al., 1976), and data back to 1880 based on estimates from the National Oceanic

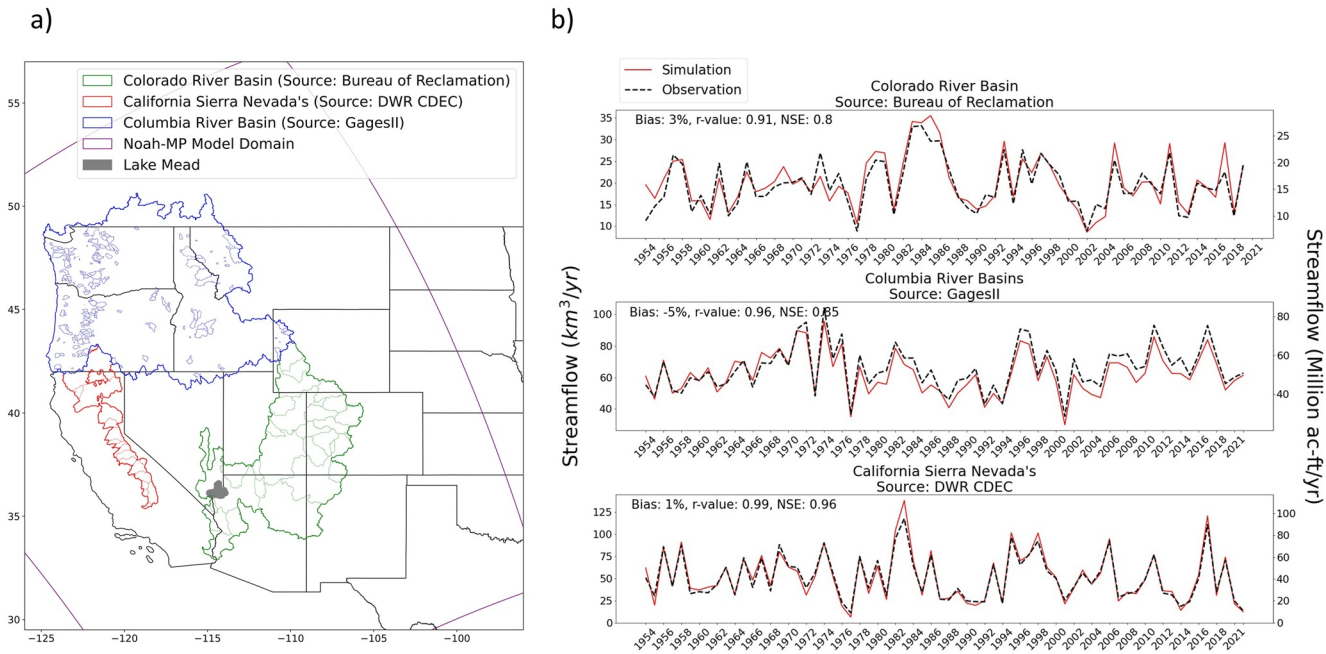

Figure 1. (a) Noah Multiparameterization modeling domain (purple outline), including the outline of major riverine basins evaluated for their runoff sensitivity (% °C^{-1}). Subbasins with observed data that were used for calibration in each major riverine basin are additionally shown. (b) Total annual streamflow from the *Baseline* simulation compared against observational data in each major riverine basin from 1954 to 2021.

and Atmospheric Administration (NOAA, 2021). For reference, the CO_2 concentrations for the years 1880, 1950, and 2021 are 285, 313, and 416 ppm. The domain-wide annual CO_2 was defined for each year in Noah-MP's MPTABLE.TBL file and each year was simulated individually with a warm start condition based on the previous year's last time-step.

In Figure 1b, we compare Noah-MP's simulated streamflow to observational data for major riverine basins across the western US that fall within our domain (Colorado River Basin, Columbia River Basin, California's Sierra Nevada). The Nash-Sutcliffe Efficiency (NSE, J. E. Nash & Sutcliffe, 1970) was used as a performance metric of monthly streamflow for Noah-MP. While all major basins are well represented, we primarily focus on the Colorado Basin due to its relatively heightened runoff sensitivity (% °C^{-1}) (later discussed). The Colorado River Basin has an NSE of 0.8 with a 3% wet bias when compared against monthly observed natural flow. The simulated snow water equivalent (SWE) is additionally validated against Snow Telemetry (SNOTEL) station data and gridded SWE (Parameter-elevation Regressions on Independent Slopes Model developed at the University of Arizona (PRISM-UA), Zeng et al., 2018) from water years 1982–2019 when PRISM-UA and SNOTEL both have data. Based on the 152 SNOTEL sites (Figure S1 in Supporting Information S1) in the Colorado Basin, our Noah-MP simulation has a −11.7% mean climatological bias compared to SNOTEL and a 4.5% wet bias compared against gridded SWE from PRISM-UA for grid cells co-located with the SNOTEL sites (Figure S1 in Supporting Information S1).

Here, we maintained the default vegetation properties based on USGS 30 arc-second 24-category land use and vegetation data (USGS, 2018). To evaluate our *Baseline* model's representation of LAI, we compared against Moderate-Resolution Imaging Spectroradiometer (MODIS) LAI observations (available from 1 January 2000–31 December 2020, Yuan et al., 2011, 2020). In comparing against this product, which has a native resolution of 0.05°, we regridded the dataset to our domain's 9 km grid. For the Colorado Basin, the simulated linear trend in annual mean LAI (from 2000 to 2020) of 10.2% is in near agreement with the 10.9% trend from MODIS LAI observations (Yuan et al., 2020) (Figure S2 in Supporting Information S1). However, based on our simulation, the Colorado Basin has a positive climatological bias of 0.47 m^2/m^2 (unit represents leaf area per land unit area). Nonetheless, this bias is reduced from 0.89 m^2/m^2 when simulating Noah-MP with its default solvers that do not consider dynamic vegetation and transient CO_2, resulting in our LAI bias falling within the uncertainty (RMSE and standard deviation of 0.79) associated with the MODIS LAI observational dataset (Yuan et al., 2011).

Table 1
Simulations Performed

Simulation	Temperature	CO_2	Description
Baseline	Observed	Varies based on observed	Includes observed warming and observed CO_2
No Warming/CO_2	Removed warming	285 ppm	Removes Warming and CO_2
CO_2 Only	Removed warming	Varies based on observed	Removes Warming but uses observed CO_2

Note. *Baseline − No Warming/CO_2* = Overall anthropogenic warming and CO_2 impact; *Baseline − CO_2 Only* = Impact of Anthropogenic Warming; *CO_2 Only − No Warming/CO_2* = Impact of CO_2.

2.2. Simulations Performed

A total of three simulations were performed in this study to evaluate runoff sensitivity (% $°C^{-1}$) and the vegetation response to CO_2. These include the *Baseline* simulation which includes warming and transient CO_2 (results from which are shown in Figure 1), a *No Warming/CO_2* simulation which removes anthropogenic warming since 1880 and uses 1880 CO_2 levels in Noah-MP, and a simulation with increasing CO_2 but anthropogenic warming removed (*CO_2 Only*). These simulations are listed in Table 1 and a time-series of the experiments temperature and CO_2 forcings is included in Figure S3 in Supporting Information S1. The simulations are used to (a) isolate the impact of the vegetation response to CO_2 (*CO_2 Only − No Warming/CO_2*), (b) isolate the impact of warming (*Baseline − CO_2 Only*), and (c) determine the overall combined impact of warming and CO_2 increases (*Baseline − No Warming/CO_2*).

We remove anthropogenic warming based on a non-linear (natural cubic spline) fit to each grid cell and each month of the ensemble mean from a suite of selected GCMs. The ensemble mean of the GCMs was used, rather than the observed temperature trend, to suppress natural variability effects in the fit (e.g., Hegerl et al., 2007). While the observed trend is dominated by anthropogenic forcing in recent decades, annual to decadal temperature fluctuations influenced temperature throughout the twentieth century (e.g., Delworth & Mann, 2000) and natural variability was relatively more important in early century warming which we additionally consider in this study (e.g., Stott et al., 2000). The GCMs were selected based on their ability to represent Northern Hemisphere warming trends across the historical period. The selection was performed by removing GCMs with significantly different Northern Hemisphere temperature trends ($p < 0.05$) when compared against observed Northern Hemisphere temperature trends from 1880–1950 to 1950–2014 (Figure S4 in Supporting Information S1). Two datasets were used to represent observed Northern Hemisphere temperature trends: Berkeley Earth Surface Temperatures (BEST; Rohde & Hausfather, 2020; BEST, 2021) and the Goddard Institute of Space Studies Surface Temperature Analysis (GISTEMP v4; Lenssen et al., 2019). A total of 15 GCMs were selected (Figure S4 in Supporting Information S1). If a GCM had multiple realizations, the mean temperature of those realizations was used to represent its temperature, consistent with our effort to suppress natural variability effects. The GCMs were bilinearly interpolated to the 9 km WRF-generated forcing data and Noah-MP resolution, and their mean was taken to obtain a single time-series for a given grid-cell. A non-linear fit was performed for each 9-km grid cell and each calendar month, which was then applied to remove anthropogenic warming from the original ERA5-WRF temperature. The mean GCM annual temperature time-series is shown in Figure 2a when averaged across the Colorado Basin. Note, a bias correction of the GCMs temperature time-series to match the observational mean does not have an impact on our results since we detrend the observed ERA5-WRF data using the slope of the fit trend (intercept term not relevant).

Although linear trends are commonly used to represent the anthropogenic effect, the non-linear fit provides a more accurate depiction of anthropogenic cooling and warming phases that have occurred from 1880 to present (Figure S5 in Supporting Information S1). To our knowledge, the non-linear trend in anthropogenically forced changes in temperature has not been used to evaluate impacts on runoff or streamflow. However, Williams et al. (2015) used a similar approach for evaluating how non-linear increases in anthropogenically forced temperature have impacted potential evapotranspiration (PET) and the Palmer Drought Severity Index throughout California. Similar to Williams et al. (2015), we found that a linear trend underestimates the anthropogenic effect on temperature, particularly in recent decades (Figure S5 in Supporting Information S1). In our study, we use a natural cubic spline, rather than a cubic polynomial fit, to prevent overfitting (e.g., Wongsai et al., 2017) to the residual natural interannual variability that is present even after averaging over all the GCMs. Figure 2b shows the

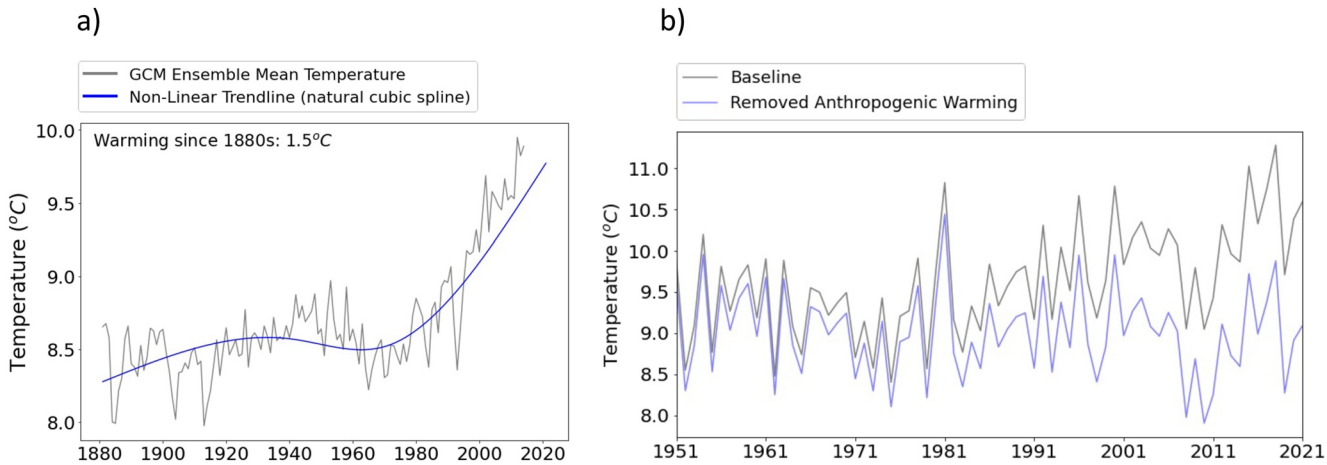

Figure 2. (a) Non-linear fit to temperature based on the suite of selected Global Climate Models (GCMs) and (b) temperature time-series for baseline (observed ERA5-WRF) conditions and when anthropogenic warming is removed. Both show temperature as the annual mean across the Colorado Basin.

baseline ERA5-WRF temperature time-series and the time-series when anthropogenic warming is removed. The time-series without warming includes the removal of the non-linear fit to the GCM data from 1951 to 2021, and is additionally shifted based on warming that occurred from 1880 to 1950. As such, anthropogenic warming since the 1880s (or roughly the pre-industrial era) is accounted for in our simulations where warming was removed.

3. Results

3.1. Runoff Sensitivity to Experiments

The general impact on runoff due to historical changes in anthropogenic warming and CO_2 is shown in Figure 3. This shows a time-series of historically simulated yearly runoff from *Baseline* (observed) conditions and when warming and CO_2 are removed (Figure 3a). Unlike the non-linear fit used to remove anthropogenic warming from the ensemble mean of several GCMs, the long term change in runoff is assessed using a linear trend fit to each experiment (Figure 3a). Based on the linear trend, total runoff since 1954 has decreased by 1.2 km^3 (0.97 MAF) or 5.7%, while without the influence of warming and CO_2 since the pre-industrial era, runoff would have increased by 0.9 km^3 (0.73 MAF) or 4.6%. Based on the difference between these two simulations, there has been an overall decrease of 2.1 km^3 (1.7 MAF), equal to a 10.3% decrease, in runoff due to anthropogenic warming and CO_2.

We also demonstrate in Figure 3b, the decadal decreases in runoff for the Colorado Basin and two major riverine basins in the western US (California Sierra Nevada and the Columbia River Basin). The percent runoff decrease

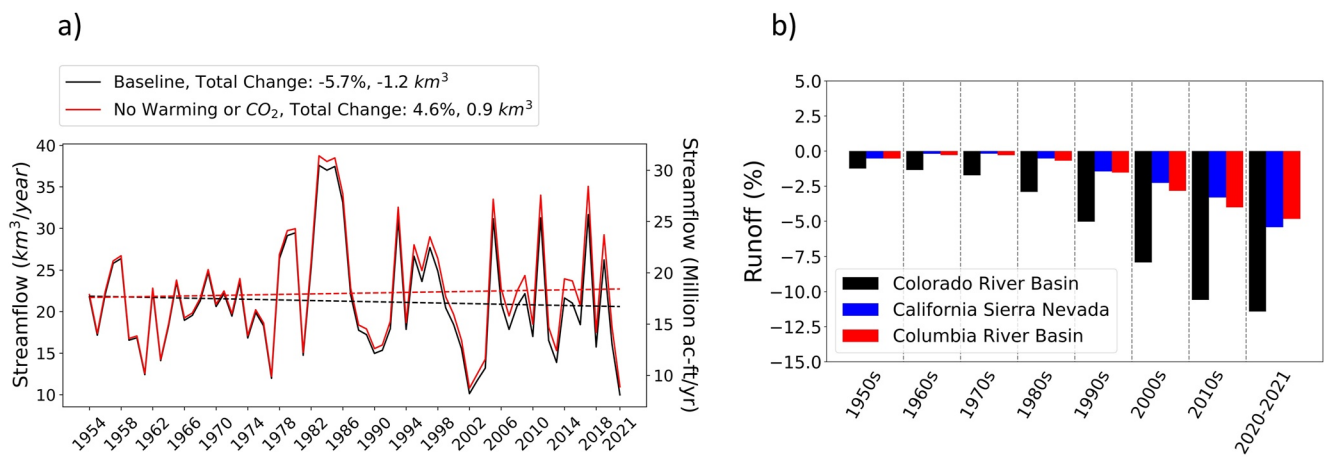

Figure 3. (a) Time-series of total annual runoff from the Colorado Basin for the *Baseline* simulation and simulation without warming/CO_2. (b) Colorado Basin's decadal runoff decrease (%) due to combined effects of warming and CO_2 compared to other major riverine basins in the western United States.

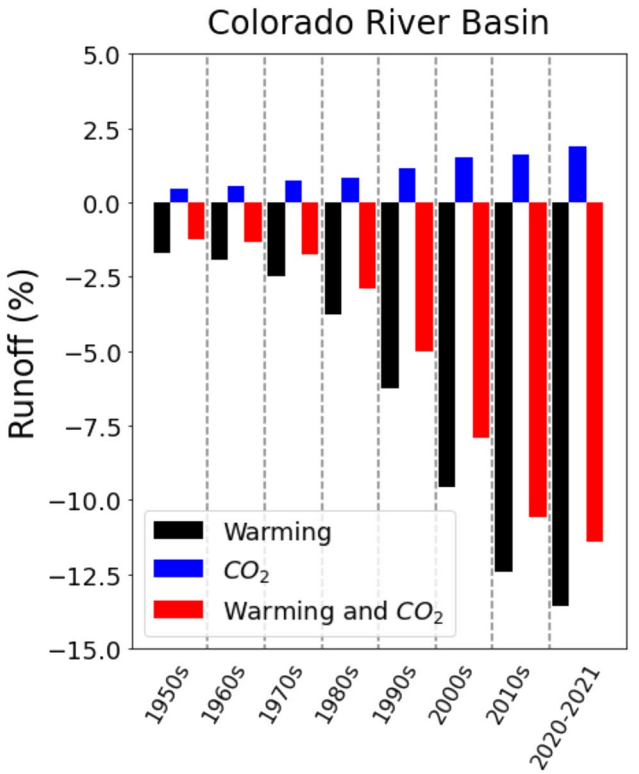

Figure 4. The percent changes in runoff from warming, CO_2, and the combination of warming and CO_2 on runoff, by decade. Warming and CO_2 impact obtained from simulations: *Baseline* − *No Warming/CO_2*; Warming impact obtained from simulations: *Baseline* − *CO_2 Only*; CO_2 impact obtained from simulations: *CO_2 Only* − *No Warming/CO_2*.

for each decade is based on the difference between the *Baseline* Simulation's mean runoff and the *No Warming/CO_2* simulation's mean runoff for each decade. This figure highlights why we focus on the Colorado Basin, which has a runoff sensitivity to the combined effects of anthropogenic warming and CO_2 i.e., nearly double that of other major western US basins.

To understand the impact of warming and CO_2 individually, as well as the combination thereof, we further break down the contributions of each factor in Figure 4. Figure 4 demonstrates the percent difference in mean runoff for each decade (similar to Figure 3b); however, here, the impact due to warming, CO_2, and warming and CO_2 is broken down. The difference in the decadal mean runoff between the experiments *Baseline* and *CO_2 Only* was used to determine warming's individual impact, the difference in runoff between experiments *CO_2 Only* and *No Warming/CO_2* was used to obtain CO_2's individual impact, and the difference in runoff between experiments *Baseline* and *No Warming/CO_2* was used to determine the overall impact of warming and CO_2 (reference Table 1 for experiment descriptions). Since the simulations are forced by the same precipitation time series, the percent differences represent changes in runoff efficiency (runoff divided by precipitation). As demonstrated in Figure 4, warming has a relatively large impact on runoff compared to CO_2; however, the ameliorating effect of CO_2 is clearly shown by the positive increase in runoff when evaluating CO_2's individual impact. We also evaluated whether the interaction between warming and CO_2 plays an important role by comparing the overall impact of warming and CO_2 on runoff (from the difference in the *Baseline* and *No/Warming CO_2* experiments) to the sum of the individual impact from CO_2 and the individual impact from warming. However, this interaction term, which increases over the simulation period, has a negligible impact on runoff for even the most recent decade (less than 0.25%).

In addition to evaluating the percent change in decadal runoff caused by anthropogenic warming and CO_2 changes, we determined the runoff sensitivity (% $°C^{-1}$). The runoff sensitivity was obtained by simply taking the difference between the overall change in runoff between each respective experiment normalized by the overall temperature change in the Colorado Basin. For example, as previously described, we found an overall decrease of 2.1 km^3 (1.7 MAF, 10.3%) in runoff that was calculated based on the difference in the total change in runoff for each experiment (*Baseline* and *No Warming/CO_2*) from the linear trends shown in Figure 3a. This overall change in runoff was then normalized by the overall anthropogenic change in temperature (1.5°C) to obtain a sensitivity of −6.8% $°C^{-1}$. Without considering the vegetation response to CO_2, Colorado Basin's runoff has a sensitivity of −8.1% $°C^{-1}$ (Table 2, included in imperial units in Table S2 in Supporting Information S1), which is in the mid- to higher-range of previous studies (McCabe & Wolock, 2007; P. C. D. Milly & Dunne, 2020; Vano et al., 2012). This indicates the vegetation response to CO_2, which results in an overall increased water use efficiency, dampens the runoff sensitivity by roughly 15%.

These results suggest that over the recent historical period, decreases in transpiration due to stomatal closure, which occurs in response to CO_2 increases, generally outweigh any increases in transpiration due to greening. In Figure 5, we break down how different variables that impact ET change from 1954 to 2021 based on the difference between the *Baseline* and *No Warming/CO_2* experiments. As demonstrated in this figure, the overall transpiration in the *Baseline* experiment is lower owing to stomatal closure outweighing the influence increasing LAI has on transpiration. However, since the increase in evaporation due to warming is greater than decreases in transpiration, there is an overall increase in ET. Our Figure 5 results agree with Figure 4, which shows that if only warming is considered the runoff reductions would have been greater due to less of an offset in ET caused by stomatal closure when both warming and CO_2 are considered.

When including warming and increasing CO_2, the Colorado Basin has volumetric sensitivity of −1.4 km^3 $°C^{-1}$. Due to overall warming and CO_2 changes since 1880, the basin is currently experiencing annual runoff that is

Table 2
Runoff Sensitivity to Warming, CO_2, and the Combination of Warming and CO_2 for the Entire Colorado Basin, and When Separated by Its Drainage Area With and Without Snowpack

	Sensitivity[c] (% °C^{-1})	Sensitivity (km^3 °C^{-1})	Sensitivity to warming since 1880[d] (%)	Sensitivity to warming since 1880 (km^3)	Baseline mean (km^3)
Warming Only	−8.1	−1.7	−12.2	−2.5	-
CO_2 Only	1.3	0.3	1.9	0.4	-
			Warming and CO_2		
Entire Basin	−6.8	−1.4	−10.3	−2.1	21.2
Regions with snowpack[a]	−7.7	−1.2	−11.6	−1.8	16.8
Regions without snowpack[b]	−4.0	−0.2	−6.0	−0.3	4.5

Note. Shown as imperial units in Table S2 in Supporting Information S1.
[a]Represents 30.9% of basin area based on a Mean Peak SWE >50 mm. [b]Represents 69.1% of basin area based on a Mean Peak SWE >50 mm. [c]Sensitivity (% °C^{-1}) based on difference in last value of linear trend fit to annual runoff for the different experiments performed (e.g., Figure 3a) divided by the overall change in temperature. [d]Sensitivity to Warming since 1880 based on difference in last value of linear trend fit to annual runoff for the different experiments performed.

2.1 km^3 (1.7 MAF) lower than in 1880 (Table 2). This is a substantial reduction, given the basin's climatological mean runoff (from 1954 to 2021) is only 21.2 km^3 (17.19 MAF). It is possible that changes in runoff efficiency are sensitive to the overall hydrologic state of the system, creating for example, a larger impact of anthropogenic warming and CO_2 on runoff during the recent prolonged drought. However, we find that this is not the case. This is demonstrated by the nearly linear relationship between warming and decreasing runoff efficiency (and peak integrated SWE) (Figure 6). Given this linear relationship, the proportionate response of runoff (to muted and then accelerating warming) is apparent in Figure 7. Here increases in anthropogenic warming are shown adjacent to changes in runoff and peak integrated SWE by decade. As demonstrated in this figure, aerosol cooling from the 1940s–1970s offsets the warming that occurred since the 1880s, keeping runoff reductions below 3% until the 1980s. However, as warming accelerated in the past few decades, reductions in runoff and SWE also accelerated.

3.2. The 2000–2021 and 2020–2021 WY Droughts

The short duration, high intensity 2020–2021 drought, and the longer, prolonged megadrought since 2000, of which it is a continuation led the US Federal Government to declare a water shortage for the first time in Colorado Basin's history on August 2021 (Bureau of Reclamation, 2022). The declaration required that Arizona, Nevada, and Mexico receive a cumulative water delivery reduction of roughly 0.756 km^3 (613,000 acre-feet) during late 2021 to early 2022 (Stern & Sheikh, 2022). Given the impacts of the 2000–2021 megadrought and the short duration, high-intensity 2020–2021 drought, we evaluate these events water budget anomalies and reductions due to anthropogenic warming and CO_2 in further detail.

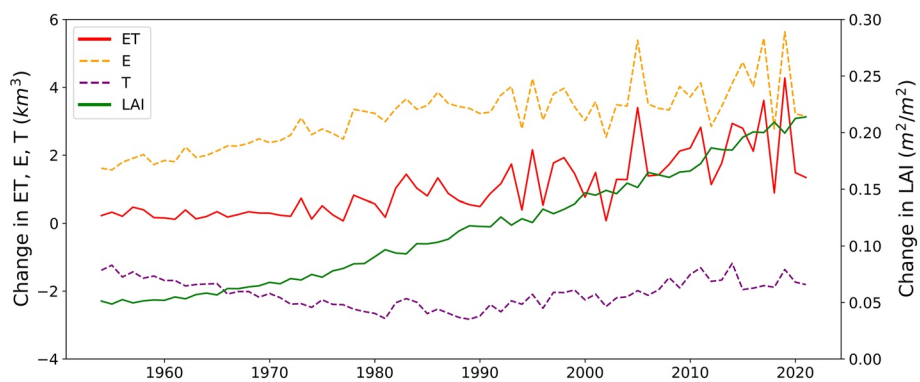

Figure 5. Annual change in evapotranspiration, evaporation (E), transpiration (T), and leaf area index summed over the Colorado Basin due to warming and CO_2 increases (simulations: *Baseline − No Warming/CO_2*).

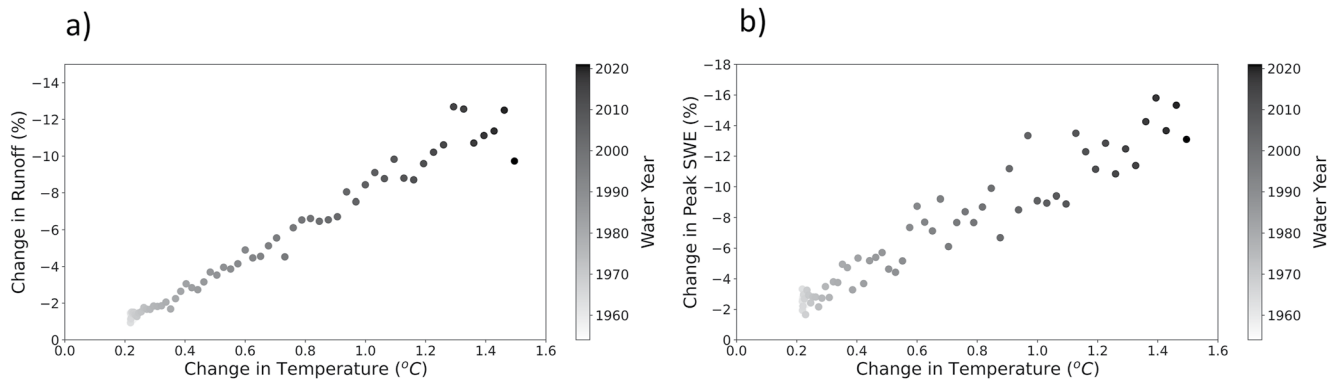

Figure 6. This figure demonstrates the approximately linear relationship between increasing temperature and decreasing (a) runoff and (b) peak integrated SWE, when summed over the Colorado Basin for each year.

Table 3 outlines the magnitude and percent anomaly in precipitation, temperature, runoff, peak integrated SWE, and ET during each of these droughts compared to the climatological mean across our simulation period (from 1954 to 2021). The same table is included in imperial units (million acre-feet) in Supporting Information S1 (Table S3 in Supporting Information S1). Observed conditions are based on the ERA5-WRF forcing across the Colorado Basin and resulting land surface variables represented by the Noah-MP *Baseline* simulation. Since the 2000–2021 years are included in the climatological mean, the precipitation during the 2000–2021 megadrought was only 3.1% lower and the temperature was only 5% (0.48°C) higher than the climatological mean. However, the runoff and peak integrated SWE demonstrate larger anomalies of −9.8% and −9.6%, respectively, owing to their sensitivity to both precipitation and temperature. Compared to the climatological mean, during the shorter, but severe 2021–2022 drought, precipitation was 23.9% lower, temperature was 8.6% (0.83°C) higher, runoff was 38.6% lower, and the peak integrated SWE was 27.2% lower than climatology. Evapotranspiration during both the megadrought and 2021–2022 drought was lower than climatology due to the lower precipitation available for ET, despite increases in temperature (Table 3).

In Table 3, we additionally demonstrate the total increase/reduction in water budget variables due to anthropogenic warming and CO_2 changes during the megadrought and the 2020–2021 drought. The impact of warming and CO_2 is calculated based on the difference between the *Baseline* and *No Warming/CO_2* simulations, using the sum of a variable (e.g., runoff, ET) across the duration of the drought time-periods of interest (2000–2021, 2021–2021). From this analysis, we find that long term anthropogenic warming since the pre-industrial era has led to a total reduction in runoff or water availability of 40.1 km^3 (32.5 MAF) during the 2000–2021 megadrought, exceeding the total storage of Lake Mead 39.78 km^3 (32.24 MAF). During the 2020–2021 drought alone, runoff was reduced by 3.0 km^3 (11.4%) from what runoff would have been without warming and CO_2 increase. The difference in Colorado Basin runoff for these 2 years alone, which pushed the basin into its first shortage, is more than three times the water delivery reductions of 0.756 km^3 (0.613 MAF) that were required by the basin's first tier 1 shortage declared on August 2021 (Stern & Sheikh, 2022). Overall, these results suggest the shortage, which was triggered by reaching a Lake Mead water level of 327.66 m (1,075 ft.) (Stern & Sheikh, 2022), would likely not have occurred without anthropogenic warming.

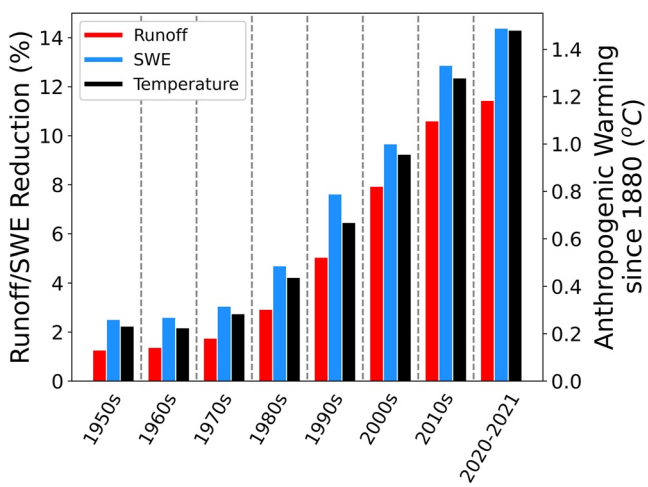

Figure 7. Reductions in runoff and peak integrated SWE, based on the overall impact of warming and CO_2, and how these reductions relate to anthropogenic warming.

The change in runoff for both the megadrought and the 2020–2021 drought was primarily driven by an increase in warming-driven ET. For the 2020–2021 drought a 13.6% reduction in runoff occurs if only warming is considered, but this is dampened somewhat by the vegetation response to CO_2 (2.2% increase in runoff if only CO_2 is considered as shown in Figure 4) resulting in a −11.4% reduction in runoff (Table 3). Peak integrated SWE was additionally reduced by 80 km^3 (11.5%) during the megadrought and 7.3 km^3 (14.4%) during the 2020–2021 WY drought due to warming, with negligible sensitivity to the CO_2 increase.

Table 3
The 2000–2021 and 2020–2021 Droughts and Their Anomaly From 1954 to 2021 Climatology (First Three Columns) and Impact From Warming/CO_2 on Water Budget Variables During the Droughts (Last Two Columns)

	Observed conditions[a]			Change due to warming, CO_2[b]	
	Anomaly[c]	Climatological mean (1954–2021)	Difference from climatology (%)	Total difference during drought[d]	Difference (%)
			2000–2021		
Precipitation (km^3)	−5.84	186.9	−3.13	-	-
Temperature (°C)	0.48	9.67	4.96	1.15	11.3
Runoff (km^3)	−2.08	21.2	−9.8	−40.1	−9.5
Peak SWE (km^3)	−3.35	34.9	−9.6	−80.0	−11.5
ET (km^3)	−1.96	164.9	−1.19	42.3	1.2
			2020–2021		
Precipitation (km^3)	−44.6	186.9	−23.9	-	-
Temperature (°C)	0.83	9.67	8.6	1.48	14.1
Runoff (km^3)	−8.2	21.2	−38.6	−3.0	−11.4
Peak SWE (km^3)	−9.5	34.9	−27.2	−7.3	−14.4
ET (km^3)	−29	164.9	−17.6	2.8	1.0

Note. Shown as imperial units (e.g., million acre-feet) in Table S3 in Supporting Information S1.
[a]Based on results from *Baseline* Simulation. [b]From difference in Simulations: *Baseline* − *No Warming/CO_2*. [c]Based on mean during drought compared to climatological mean. [d]Based on total difference for all variables except Temperature is based on mean difference.

3.3. Accelerated Reductions in Snowpack Regions

Since snowpack regions only make up roughly one third of the Colorado Basin's drainage area but supply roughly two thirds of its total runoff, we further explore the sensitivity of runoff (% $°C^{-1}$) for these vital regions. We perform this analysis by separating regions with and without seasonal snowpack based on a 50 mm historically averaged peak SWE threshold (based on our *Baseline* simulation from 1954 to 2021). Figure 8 demonstrates the sensitivity of annual runoff to warming/CO_2 for regions with snowpack (Figure 8a) and without snowpack (Figure 8b). Regions associated with snowpack show nearly double the runoff sensitivity to warming (−7.7% $°C^{-1}$) compared to regions without snowpack (−4.0% $°C^{-1}$) (Table 2). Thus, despite only making up ∼30% of the basin's drainage area, 86% of the runoff decrease is driven by water loss in snowpack regions (−1.2 km^3 $°C^{-1}$ for snowpack regions compared to 0.2 km^3 $°C^{-1}$ for regions without snowpack). Using the Budyko framework (Budyko, 1974), we demonstrate that both regions experience increases in their evaporative index (ET/P) due to warming; however, snowpack regions generally show larger increases in the evaporative index *and* aridity index (PET/P) compared to regions without snowpack (Figure 8c). (The PET was calculated based on the FAO Penman-Monteith equation [Allen, 1996].) In other words, regions associated with snowpack appear to be experiencing greater aridification relative to non-snowpack regions, and thus larger decreases in their runoff efficiency. The larger increase in aridity (larger decrease in runoff efficiency) in snowpack regions is due to warming in an energy-limited regime in the winter and likely due to reductions in albedo due to snowpack loss (P. C. D. Milly & Dunne, 2020). Due to space limitations, we provide further discussion in Supporting Information S1 regarding spatial (Figures S6 and S7 in Supporting Information S1) and seasonal changes (Figure S8 in Supporting Information S1) associated with water budget variables and how they have changed due to anthropogenic warming in the Colorado Basin's snowpack regions.

4. Uncertainties in Study

In this study, we focus on runoff's sensitivity to temperature and CO_2 given high confidence in their anthropogenically forced trends during the historical period. Although Colorado Basin runoff is sensitive to precipitation (e.g., Hoerling et al., 2019), the ensemble GCM mean precipitation changes in this basin are neutral during the historical period (IPCC AR6, 2021). Hence our analysis represents the expected anthropogenic impact on runoff

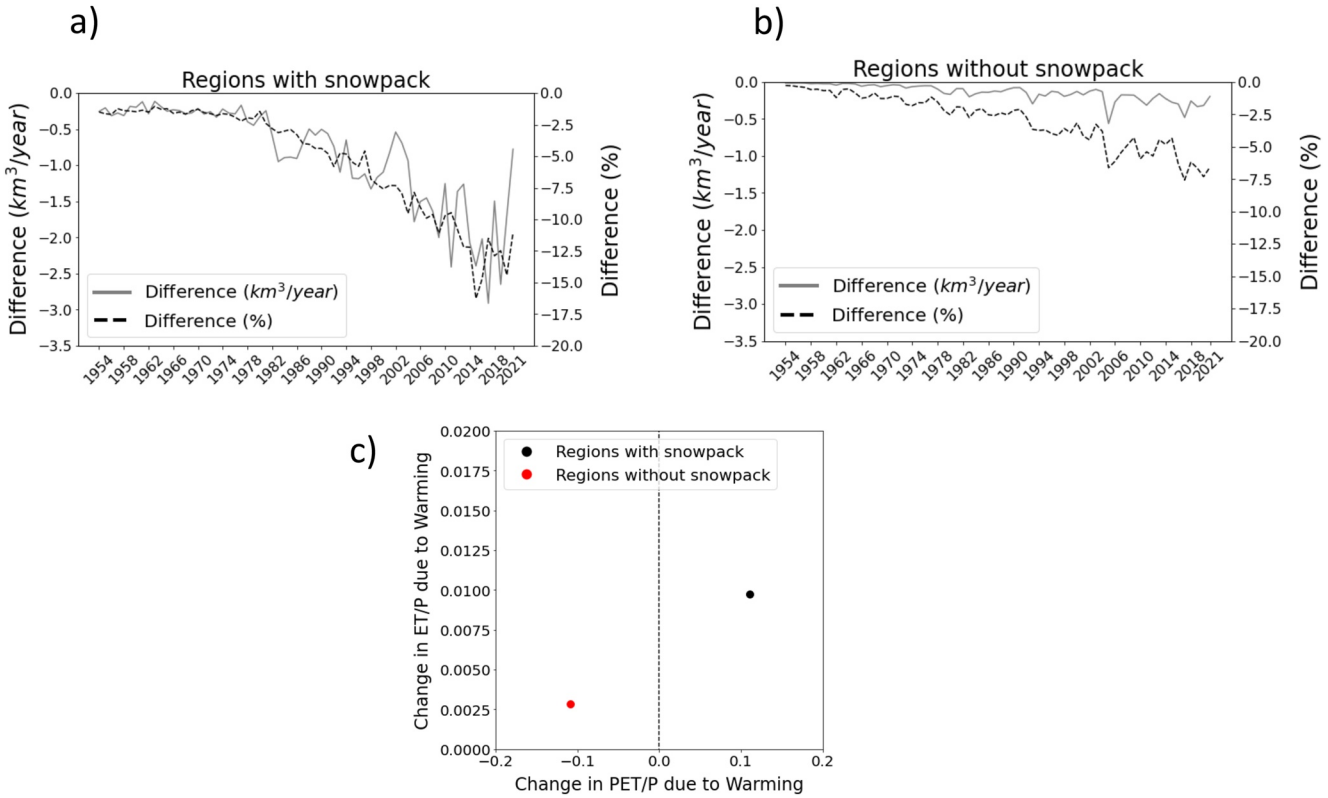

Figure 8. Annual difference in runoff (summed across the Colorado River Basin) due to warming/CO_2 for (a) regions with snowpack and (b) regions without snowpack. (c) Change in variables from Budyko Analysis (summed across the Colorado Basin) due to warming and CO_2 for regions with and without snowpack, demonstrating greater aridification associated with snowpack regions.

during the historical period as primarily driven by warming, albeit with a dampening vegetation-CO_2 response. The impact of anthropogenically forced precipitation changes across the historical period may be further explored via careful selection and downscaling of CMIP6 GCMs that resolve relevant atmospheric processes in the Colorado Basin. While anthropogenically forced changes in precipitation during the historical period are neutral based on the CMIP6 ensemble mean, the GCMs begin to agree on the sign and magnitude of the forced anthropogenic precipitation signal with further warming. Generally, slight drying prevails across the majority of the Colorado Basin with slight wetting along the edges of the Upper Colorado Basin (IPCC AR6, 2021). Therefore, studies of projected hydrologic conditions over this region should consider changes in precipitation, in addition to warming and impacts of increasing CO_2 on vegetation.

Additionally, while our study provides possibly the first evaluation of Colorado Basin's historical runoff response to CO_2, the representation of vegetation and its response to CO_2 is an active area of research. While several studies agree with our finding that CO_2-induced stomatal closure can partially offset reductions in runoff (e.g., Lian et al., 2018; Swann et al., 2016), some studies (e.g., Mankin et al., 2017; X.-Y. Zhang et al., 2022) suggest that stomatal closure and greening have a roughly compensatory effect on projected runoff changes. Two possible sources of uncertainty in our modeling approach that could impact our results include a high LAI bias and lack of a plant hydraulic scheme in the dynamic vegetation model used.

While our use of a dynamic vegetation model, rather than static vegetation conditions, substantially reduces our LAI bias into the MODIS LAI observational range of uncertainty (Yuan et al., 2011); our simulated LAI still has a high bias compared to observations. This LAI bias could have been reduced through parameter tuning of vegetation properties such as that performed in Niu et al. (2020); however, given observational uncertainties in LAI, we chose to maintain default Noah-MP vegetation parameters based on USGS 30 arc-second 24-category land use and vegetation data. Qualitatively, a positive LAI bias indicates that despite simulated streamflow closely matching observations, the simulated transpiration is likely too high. Leaf respiration, leaf turnover, and/or wilting due to cold and drought stresses associated with soil moisture conditions that are influenced by LAI and transpiration could impact the

amount of carbon assimilated for further LAI growth and stomatal closure. Generally, we expect that a high LAI bias would lead to a high bias in transpiration and as a result a bias in the amount or magnitude of stomatal closure and greening; however, we expect that the (relative) change in stomatal closure and greening in response to CO_2 are unaffected given that our trend in LAI matches the observational trend in LAI. Nonetheless, future studies should confirm that relative changes in greening and stomatal closure remain generally unaffected within a reasonable LAI bias.

In addition to a bias in LAI, our simulations do not include an explicit plant hydraulic scheme. At the time of our analysis, we employed the latest published version of WRF-Hydro (version 5.1.1) and its associated Noah-MP LSM, which includes Ball-Berry photosynthesis-based stomatal resistance (Ball et al., 1987) combined with a dynamic vegetation model (Dickinson et al., 1998). As CO_2 increases, the dynamic vegetation model represents the stomatal closure effect on transpiration and a greening effect due to carbon assimilation that leads to increased transpiration. However, in the version of Noah-MP employed, the plant water-stress factor is represented as an empirical function of soil moisture. The plant water-stress factor plays an important role in the regulation of photosynthesis and stomatal conductance, and ultimately the overall water budget due to its influence on transpiration (Niu et al., 2011). However, recent studies by Li et al. (2021) and Niu et al. (2020) have developed explicit representations of root structure and subsequent water uptake, that have been shown to represent ET more accurately and vegetations ability to uptake water during drought (e.g., Li et al., 2021; Niu et al., 2020) compared to the dynamic vegetation code we employed. Niu et al. (2020) developed and evaluated dynamic root conditions, while Li et al. (2021) evaluated a whole-plant hydraulic strategy known as the big tree concept. While the plant stomatal water stress factor is related to the plant water storage or soil moisture available for transpiration in the current version of Noah-MP used in this study as well as Li et al. (2021), in Li et al. (2021) the plant water storage is explicitly represented based on a physical representation of water fluxes throughout vegetation's roots, stems, and leaf. We recommend that future studies incorporate one or more of these explicit plant hydraulic schemes, which will likely be incorporated into upcoming versions of WRF-Hydro.

Finally, this study employs an LSM capable of representing dynamic vegetation unlike other commonly used hydrologic models such as the latest version of Variable Infiltration Capacity (Hamman et al., 2018). However, other LSM's are available that depict dynamic vegetation and could be compared against in terms of their representation of changes in runoff due to warming and CO_2, such as the Community Land Model (Lawrence et al., 2019). Since the dynamic vegetation schemes and the runoff solvers incorporated in other LSMs typically differ from Noah-MP, an evaluation on the uncertainties associated with model choice would be beneficial.

5. Conclusions

In this study, we evaluate how anthropogenic warming has impacted the Colorado River Basin's runoff or water availability by accounting for non-linear anthropogenic changes in temperature since the 1880s, and by considering possible effects of the vegetation response to increasing CO_2. Generally, we find that anthropogenic warming began to exacerbate runoff losses in the 1980s and the vegetation response to CO_2 has dampened the basin's historical runoff losses somewhat. We performed our analysis based on hydrologic simulations across the western US with the Noah MP LSM from 1954 to 2021. These simulations were driven by the ERA5 reanalysis dynamically downscaled to 9 km with WRF. Three simulations were performed: one including the effects of long term warming and CO_2 increases; one with the warming trend removed but CO_2 increases retained; and one with the warming removed and CO_2 levels set to pre-industrial levels. Using these simulations, we addressed important questions for this crucial basin, including (a) the runoff sensitivity to warming and CO_2 increases, (b) the impact of warming/CO_2 during the ongoing megadrought (2000–2021) and the shorter duration, but severe 2020–2021 drought, and (c) runoff sensitivity to warming/CO_2 for snowpack versus non-snowpack regions.

Our results suggest that increased vegetation water use efficiency (reductions in stomatal conductance, which tend to decrease transpiration) outweigh increases in greening (which tends to increase transpiration). This net decrease of transpiration due to increased CO_2 results in roughly a 15% dampening of the runoff decrease due to warming. Thus, the Colorado Basin exhibits a 6.8% $°C^{-1}$ reduction in runoff or water availability, compared to 8.1% $°C^{-1}$ if only warming is considered. We also demonstrated that runoff in snowpack regions in this basin experience roughly double the sensitivity to warming due to larger increases in aridification and evaporation compared to non-snowpack regions.

The long term impact of anthropogenic warming most notably played a role in the first water shortage in the Colorado River Basin, declared by the US government on August 2021. The severe 2020–2021 drought, and

the longer megadrought that it is a part of, that led to the water shortage were primarily driven by a large negative precipitation anomaly, attributable to internal variability (Mankin et al., 2021). However, we found that anthropogenically-driven long term warming reduced natural runoff by more than the total storage of Lake Mead from 2000 to 2021, and during the severe drought from 2020 to 2021 runoff was reduced by 3 times the water delivery reductions required from the basin's first shortage. Based on these reductions in runoff, the Colorado Basin's first water shortage likely would not have been required in 2021 without anthropogenic warming. Without reducing greenhouse gas emissions, runoff reductions will likely continue to occur as temperature increases, despite ameliorating effects of the vegetation response to CO_2.

Data Availability Statement

The CMIP6 GCM temperature data used for this study (CMIP6, 2021) are freely available from the Earth System Grid Federation (ESGF) (esgf-node.llnl.gov/search/cmip6). The observational temperature data can be obtained from the Berkeley Earth Surface Temperature (BEST) dataset (http://berkeleyearth.org/data/) and the GISS Surface Temperature Analysis ver. 4 (GISSTEMP v4) (https://data.giss.nasa.gov/gistemp/) (GISTEMP Team, 2022). The CO_2 data was obtained from the Mauna Loa Global Monitoring Observatory (https://gml.noaa.gov/ccgg/trends/data.html) (Mauna Loa Global Monitoring Observatory, 2021). Observed trends in Leaf Area Index (LAI) based on MODIS (Yuan et al., 2020) were obtained from the Land-Atmosphere Interaction Research Group at Sun Yat-sen University (http://globalchange.bnu.edu.cn/research/laiv6). Observational streamflow data used in this study are additionally available, including observed Colorado Basin streamflow data from the Bureau of Reclamation (2021) at https://www.usbr.gov/lc/region/g4000/NaturalFlow/current.html, observed California Sierra Nevada streamflow from the Department of Water Resources (2021) at https://cdec.water.ca.gov/reportapp/javareports?name=FNF, and additional GagesII natural flow streamflow data across the western United States from Falcone (2011) at https://water.usgs.gov/GIS/metadata/usgswrd/XML/gagesII_Sept2011.xml.

Acknowledgments
The lead author is supported as an Assistant Project Scientist at the UCLA Center for Climate Science. We would like to acknowledge funding from the U.S. Department of Energy, Office of Science, project "Identifying Hydrologic Cycle Changes Under Future Climate" (award no. B655147) and the California Energy Commission grant "Development of Climate Projections for California and Identification of Priority Projections" (agreement EPC-20-006). Also, we thank the Computational and Information Systems Lab at UCAR and the WRF-Hydro team for their support and feedback. We acknowledge the World Climate Research Programme's Working Group on Coupled Modeling, which is responsible for CMIP, and we thank the climate modeling groups for producing and making available their model output.

References

Allen, R. G. (1996). Assessing integrity of weather data for reference evapotranspiration estimation. *Journal of Irrigation and Drainage Engineering*, *122*(2), 97–106. https://doi.org/10.1061/(asce)0733-9437(1996)122:2(97)

American Water Works Association. (2021). U.S. declares first-ever Colorado River water shortage. Retrieved from https://www.awwa.org/AWWA-Articles/us-declares-first-ever-colorado-river-water-shortage#:~:text=An%20Aug.,due%20to%20declining%20reservoir%20levels

Ball, J. T., Woodrow, I. E., & Berry, J. A. (1987). A model predicting stomatal conductance and its contribution to the control of photosynthesis under different environmental conditions. In J. Biggins (ed.), *Progress in Photosynthesis Research* (pp. 221–224). Springer, Dordrecht. https://doi.org/10.1007/978-94-017-0519-6_48

Berkley Earth Surface Temperature (BEST). (2021). Data overview: Land + Ocean (1850-recent) [Dataset]. Berkeley Earth. Retrieved from http://berkeleyearth.org/data/

Budyko, M. I. (1974). *Climate and life* (p. 508). Academic Press.

Bureau of Reclamation. (2021). Current natural flow data 1906-2019 [Dataset]. Bureau of Reclamation. Retrieved from https://www.usbr.gov/lc/region/g4000/NaturalFlow/current.html

Bureau of Reclamation. (2022). Reclamation announces 2022 operating conditions for Lake Powell and Lake Mead. Press Release. Retrieved from https://www.usbr.gov/newsroom/#/news-release/3950

CMIP6. (2021). CMIP6 data search [Dataset]. Coupled Model Intercomparison Project (CMIP). Retrieved from https://esgf-node.llnl.gov/search/cmip6/

Delworth, T. L., & Mann, M. E. (2000). Observed and simulated multidecadal variability in the Northern Hemisphere. *Climate Dynamics*, *16*(9), 661–676. https://doi.org/10.1007/s003820000075

Department of Water Resources. (2021). California Data Exchange Center: Daily full natural flow [Dataset]. California Department of Water Resources. Retrieved from https://cdec.water.ca.gov/reportapp/javareports?name=FNF

Dickinson, R. E., Shaikh, M., Bryant, R., & Graumlich, L. (1998). Interactive canopies for a climate model. *Journal of Climate*, *11*, 2823–2836. https://doi.org/10.1175/1520-0442(1998)011<2823:ICFACM>2.0.CO;2

Falcone, J. (2011). GAGES-II: Geospatial attributes of gages for evaluating streamflow [Dataset]. United States Geological Survey. Retrieved from https://water.usgs.gov/GIS/metadata/usgswrd/XML/gagesII_Sept2011.xml

Fensholt, R., Langanke, T., Rasmussen, K., Reenberg, A., Prince, S. D., Tucker, C., et al. (2012). Greenness in semi-arid areas across the globe 1981–2007—An Earth observing satellite based analysis of trends and drivers. *Remote Sensing of Environment*, *121*, 144–158. https://doi.org/10.1016/j.rse.2012.01.017

Gillett, N. P., Kirchmeier-Young, M., Ribes, A., Shiogama, H., Hegerl, G. C., Knutti, R., et al. (2021). Constraining human contributions to observed warming since the pre-industrial period. *Nature Climate Change*, *11*(3), 207–212. https://doi.org/10.1038/s41558-020-00965-9

GISTEMP Team. (2022). GISS surface temperature analysis (GISTEMP), version 4 [Dataset]. NASA Goddard Institute for Space Studies. Retrieved from https://data.giss.nasa.gov/gistemp/

Gochis, D. J., Barlage, M., Cabell, R., Dugger, A., Fanfarillo, A., FitzGerald, K., et al. (2020). The WRF-Hydro modeling system technical description (Versions 5.1.1). NCAR Technical Note.

Hamman, J. J., Nijssen, B., Bohn, T. J., Gergel, D. R., & Mao, Y. (2018). The Variable Infiltration Capacity model version 5 (VIC-5): Infrastructure improvements for new applications and reproducibility. *Geoscientific Model Development*, *11*(8), 3481–3496. https://doi.org/10.5194/gmd-11-3481-2018

Hegerl, G. C., Zwiers, F. W., Braconnot, P., Gillett, N. P., Luo, Y., Marengo Orsini, J. A., et al. (2007). Understanding and attributing climate change. In *Climate change 2007: The physical science basis. Contribution of Working Group I to the fourth assessment report of the Intergovernmental Panel on Climate Change*. Cambridge University Press.

Hoerling, M., Barsugli, J., Livneh, B., Eischeid, J., Quan, X., & Badger, A. (2019). Causes for the century-long decline in Colorado River flow. *Journal of Climate*, *32*(23), 8181–8203. https://doi.org/10.1175/JCLI-D-19-0207.1

Hong, S.-Y., Noh, Y., & Dudhia, J. (2006). A new vertical diffusion package with an explicit treatment of entrainment processes. *Monthly Weather Review*, *134*(9), 2318–2341. https://doi.org/10.1175/MWR3199.1

Iacono, M. J., Delamere, J. S., Mlawer, E. J., Shephard, M. W., Clough, S. A., & Collins, W. D. (2008). Radiative forcing by long-lived green-house gases: Calculations with the AER radiative transfer models. *Journal of Geophysical Research*, *113*(D13), D13103. https://doi.org/10.1029/2008JD009944

IPCC AR6. (2021). In V. Masson-Delmotte, P. Zhai, A. Pirani, S. L. Connors, C. Péan, S. Berger, et al. (Eds.), *Climate change 2021: The physical science basis. Contribution of Working Group I to the sixth assessment report of the Intergovernmental Panel on Climate Change*. Cambridge University Press.

Keeling, C. D., Bacastow, R. B., Bainbridge, A. E., Ekdahl, C. A., Guenther, P. R., Waterman, L. S., & Chin, J. F. S. (1976). Atmospheric carbon dioxide variations at Mauna Loa Observatory, Hawaii. *Tellus*, *28*(6), 538–551. https://doi.org/10.1111/j.2153-3490.1976.tb00701.x

Lawrence, D. M., Fisher, R. A., Koven, C. D., Oleson, K. W., Swenson, S. C., Bonan, G., et al. (2019). The Community Land Model version 5: Description of new features, benchmarking, and impact of forcing uncertainty. *Journal of Advances in Modeling Earth Systems*, *11*(12), 4245–4287. https://doi.org/10.1029/2018MS001583

Lehner, F., Wahl, E. R., Wood, A. W., Blatchford, D. B., & Llewellyn, D. (2017). Assessing recent declines in Upper Rio Grande runoff efficiency from a paleoclimate perspective. *Geophysical Research Letters*, *44*(9), 4124–4133. https://doi.org/10.1002/2017GL073253

Lenssen, N., Schmidt, G., Hansen, J., Menne, M., Persin, A., Ruedy, R., & Zyss, D. (2019). Improvements in the GISTEMP uncertainty model. *Journal of Geophysical Research: Atmospheres*, *124*(12), 6307–6326. https://doi.org/10.1029/2018JD029522

Li, L., Yang, Z.-L., Matheny, A. M., Zheng, H., Swenson, S. C., Lawrence, D. M., et al. (2021). Representation of plant hydraulics in the Noah-MP land surface model: Model development and multiscale evaluation. *Journal of Advances in Modeling Earth Systems*, *13*(4), e2020MS002214. https://doi.org/10.1029/2020MS002214

Lian, X., Piao, S., Huntingford, C., Li, Y., Zeng, Z., Wang, X., et al. (2018). Partitioning global land evapotranspiration using CMIP5 models constrained by observations. *Nature Climate Change*, *8*(7), 640–646. https://doi.org/10.1038/s41558-018-0207-9

Mankin, J. S., Seager, R., Smerdon, J. E., Cook, B. I., & Williams, A. P. (2019). Mid-latitude freshwater availability reduced by projected vegetation responses to climate change. *Nature Geoscience*, *12*(12), 983–988. https://doi.org/10.1038/s41561-019-0480-x

Mankin, J. S., Simpson, I., Hoell, A., Fu, R., Lisonbee, J., Sheffield, A., & Barrie, D. (2021). *NOAA drought task force report on the 2020-2021 Southwestern U.S. drought*. NOAA Drought Task Force, MAPP, and NIDIS.

Mankin, J. S., Smerdon, J. E., Cook, B. I., Williams, A. P., & Seager, R. (2017). The curious case of projected twenty-first-century drying but greening in the American West. *Journal of Climate*, *30*(21), 8689–8710. Retrieved from https://journals.ametsoc.org/view/journals/clim/30/21/jcli-d-17-0213.1.xml. https://doi.org/10.1175/jcli-d-17-0213.1

Mauna Loa Global Monitoring Observatory. (2021). Trends in atmospheric carbon dioxide [Dataset]. National Oceanic and Atmospheric Administration. Retrieved from https://gml.noaa.gov/ccgg/trends/data.html

McCabe, G. J., & Wolock, D. M. (2007). Warming may create substantial water supply shortages in the Colorado River basin. *Geophysical Research Letters*, *34*(22), L22708. https://doi.org/10.1029/2007GL031764

Milly, P. C., & Dunne, K. A. (2016). Potential evapotranspiration and continental drying. *Nature Climate Change*, *6*(10), 946–949. https://doi.org/10.1038/nclimate3046

Milly, P. C. D., & Dunne, K. A. (2020). Colorado River flow dwindles as warming-driven loss of reflective snow energizes evaporation. *Science*, *367*(6483), 1252–1255. https://doi.org/10.1126/science.aay9187

Morrison, H., & Milbrandt, J. (2015). Parameterization of cloud microphysics based on the prediction of bulk ice particle properties. Part I: Scheme description and idealized tests. *Journal of the Atmospheric Sciences*, *72*(1), 287–311. https://doi.org/10.1175/JAS-D-14-0065.1

Mote, P. W., Li, S., Lettenmaier, D. P., Xiao, M., & Engel, R. (2018). Dramatic declines in snowpack in the western US. *npj Climate and Atmospheric Science*, *1*, 2. https://doi.org/10.1038/s41612-018-0012-1

Nash, J. E., & Sutcliffe, J. V. (1970). River flow forecasting through conceptual models part I — A discussion of principles. *Journal of Hydrology*, *10*(3), 282–290. https://doi.org/10.1016/0022-1694(70)90255-6

Nash, L. L., & Gleick, P. H. (1991). Sensitivity of streamflow in the Colorado basin to climatic changes. *Journal of Hydrology*, *125*(3), 221–241. https://doi.org/10.1016/0022-1694(91)90030-1

National Oceanic and Atmospheric Administration. (2021). Climate change: Atmospheric carbon dioxide. Retrieved from https://www.climate.gov/news-features/understanding-climate/climate-change-atmospheric-carbon-dioxide

NCAR. (2022). Noah-multiparameterization land surface model (Noah-MP LSM) [Dataset]. Retrieved from https://ral.ucar.edu/solutions/products/noah-multiparameterization-land-surface-model-noah-mp-lsm

Niu, G.-Y., Fang, Y.-H., Chang, L.-L., Jin, J., Yuan, H., & Zeng, X. (2020). Enhancing the Noah-MP ecosystem response to droughts with an explicit representation of plant water storage supplied by dynamic root water uptake. *Journal of Advances in Modeling Earth Systems*, *12*(11), e2020MS002062. https://doi.org/10.1029/2020MS002062

Niu, G.-Y., Yang, Z.-L., Mitchell, K. E., Chen, F., Ek, M. B., Barlage, M., et al. (2011). The community Noah land surface model with multiparameterization options (Noah-MP): 1. Model description and evaluation with local-scale measurements. *Journal of Geophysical Research*, *116*(D12), D12109. https://doi.org/10.1029/2010JD015139

Piao, S., Wang, X., Park, T., Chen, C., Lian, X., He, Y., et al. (2020). Characteristics, drivers and feedbacks of global greening. *Nature Reviews Earth & Environment*, *1*, 14–27. https://doi.org/10.1038/s43017-019-0001-x

Rahimi, S., Krantz, W., Lin, Y.-H., Bass, B., Goldenson, N., Hall, A., et al. (2022). Evaluation of a reanalysis-driven configuration of WRF4 over the western United States from 1980 to 2020. *Journal of Geophysical Research: Atmospheres*, *127*(4), e2021JD035699. https://doi.org/10.1029/2021JD035699

Rohde, R. A., & Hausfather, Z. (2020). The Berkeley Earth Land/Ocean Temperature Record (BEST) [Dataset]. Earth System Science Data, *12*(4), 3469–3479. https://doi.org/10.5194/essd-12-3469-2020. Retrieved from http://berkeleyearth.org/data/

Schwartz, S. E., & Andreae, M. O. (1996). Uncertainty in climate change caused by aerosols. *Science*, *272*(5265), 1121. https://doi.org/10.1126/science.272.5265.1121

Stern, C. V., & Sheikh, P. A. (2022). Congressional research service, 2022. Management of the Colorado River: Water allocations, drought, and the federal role. Retrieved from https://crsreports.congress.gov

Stott, P. A., Tett, S. F. B., Jones, G. S., Allen, M. R., Mitchell, J. F. B., & Jenkins, G. J. (2000). External control of 20th century temperature by natural and anthropogenic forcings. *Science*, *290*(5499), 2133–2137. https://doi.org/10.1126/science.290.5499.2133

Swann, A. L., Hoffman, F. M., Koven, C. D., & Randerson, J. T. (2016). Plant responses to increasing CO_2 reduce estimates of climate impacts on drought severity. *Proceedings of the National Academy of Sciences*, *113*(36), 10019–10024. https://doi.org/10.1073/pnas.1604581113

Tiedtke, M. (1989). A comprehensive mass flux scheme for cumulus parameterization in large-scale models. *Monthly Weather Review*, *117*(8), 1779–1800. https://doi.org/10.1175/1520-0493(1989)117<1779:ACMFSF>2.0.CO;2

Udall, B., & Overpeck, J. (2017). The twenty-first century Colorado River hot drought and implications for the future. *Water Resources Research*, *53*(3), 2404–2418. https://doi.org/10.1002/2016WR019638

USGS. (2018). Global land cover characterization (GLCC) [Dataset]. USGS EROS archive - Land Cover Products. https://doi.org/10.5066/F7GB230D

Vano, J. A., Das, T., & Lettenmaier, D. P. (2012). Hydrologic sensitivities of Colorado River runoff to changes in precipitation and temperature. *Journal of Hydrometeorology*, *13*(3), 932–949. https://doi.org/10.1175/JHM-D-11-069.1

Wilcox, L. J., Highwood, E. J., & Dunstone, N. J. (2013). The influence of anthropogenic aerosol on multi-decadal variations of historical global climate. *Environmental Research Letters*, *8*, 2. https://doi.org/10.1088/1748-9326/8/2/024033

Williams, A. P., Cook, B. I., & Smerdon, J. E. (2022). Rapid intensification of the emerging southwestern North American megadrought in 2020–2021. *Nature Climate Change*, *12*(3), 232–234. https://doi.org/10.1038/s41558-022-01290-z

Williams, A. P., Cook, E. R., Smerdon, J. E., Cook, B. I., Abatzoglou, J. T., Bolles, K., et al. (2020). Large contribution from anthropogenic warming to an emerging North American megadrought. *Science*, *368*(6488), 314–318. https://doi.org/10.1126/science.aaz9600

Williams, A. P., Seager, R., Abatzoglou, J. T., Cook, B. I., Smerdon, J. E., & Cook, E. R. (2015). Contribution of anthropogenic warming to California drought during 2012–2014. *Geophysical Research Letters*, *42*(16), 6819–6828. https://doi.org/10.1002/2015GL064924

Wongsai, N., Wongsai, S., & Huete, A. R. (2017). Annual seasonality extraction using the cubic spline function and decadal trend in temporal daytime MODIS LST data. *Remote Sensing*, *9*(12), 1254. https://doi.org/10.3390/rs9121254

Xiao, M., Udall, B., & Lettenmaier, D. P. (2018). On the causes of declining Colorado River streamflows. *Water Resources Research*, *54*(9), 6739–6756. https://doi.org/10.1029/2018WR023153

Yang, Y., Roderick, M. L., Zhang, S., McVicar, T. R., & Donohue, R. J. (2019). Hydrologic implications of vegetation response to elevated CO_2 in climate projections. *Nature Climate Change*, *9*(1), 44–48. https://doi.org/10.1038/s41558-018-0361-0

Yuan, H., Dai, Y., & Li, S. (2020). Reprocessed MODIS Version 6 Leaf Area Index data sets for land surface and climate modelling [Dataset]. Sun Yat-sun University. Retrieved from http://globalchange.bnu.edu.cn/research/laiv6

Yuan, H., Dai, Y., Xiao, Z., Ji, D., & Shangguan, W. (2011). Reprocessing the MODIS Leaf Area Index products for land surface and climate modelling. *Remote Sensing of Environment*, *115*(5), 1171–1187. https://doi.org/10.1016/j.rse.2011.01.001

Zeng, X., Broxton, P., & Dawson, N. (2018). Snowpack change from 1982 to 2016 over conterminous United States. *Geophysical Research Letters*, *45*(23), 12940–12947. https://doi.org/10.1029/2018GL079621

Zhang, C., Wang, Y., & Hamilton, K. (2011). Improved representation of boundary layer clouds over the southeast Pacific in ARW-WRF using a modified Tiedtke cumulus parameterization scheme. *Monthly Weather Review*, *139*(11), 3489–3513. https://doi.org/10.1175/MWR-D-10-05091.1

Zhang, X.-Y., Jin, J., Zeng, X., Hawkins, C. P., Neto, A. A. M., & Niu, G.-Y. (2022). The compensatory CO_2 fertilization and stomatal closure effects on runoff projection from 2016–2099 in the western United States. *Water Resources Research*, *58*(1), e2021WR030046. https://doi.org/10.1029/2021WR030046

Zhu, Z., Piao, S., Lian, X., Myneni, R. B., Peng, S., & Yang, H. (2017). Attribution of seasonal leaf area index trends in the northern latitudes with "optimally" integrated ecosystem models. *Global Change Biology*, *23*(11), 4798–4813. https://doi.org/10.1111/gcb.13723

References From the Supporting Information

Bass, B., Rahimi, S., Goldenson, N., Hall, A., Norris, J., & Lebow, Z. J. (2023). Achieving realistic runoff in the western United States with a land surface model forced by dynamically downscaled meteorology. *Journal of Hydrometeorology*, *24*(2), 269–283. https://doi.org/10.1175/JHM-D-22-0047.1

Cai, X., Yang, Z.-L., David, C. H., Niu, G.-Y., & Rodell, M. (2014). Hydrological evaluation of the Noah-MP land surface model for the Mississippi River Basin. *Journal of Geophysical Research: Atmospheres*, *119*(1), 23–38. https://doi.org/10.1002/2013JD020792

Cuntz, M., Mai, J., Samaniego, L., Clark, M., Wulfmeyer, V., Branch, O., et al. (2016). The impact of standard and hard-coded parameters on the hydrologic fluxes in the Noah-MP land surface model. *Journal of Geophysical Research: Atmospheres*, *121*(10), 676–700. https://doi.org/10.1002/2016JD025097

Gochis, D. J., Yates, D., Sampson, K., Dugger, A., McCreight, J., Barlage, M., et al. (2019). Overview of national water model calibration: General strategy and optimization. Retrieved from https://ral.ucar.edu/sites/default/files/public/9_RafieeiNasab_CalibOverview_CUAHSI_Fall019_0.pdf

Lian, X., Piao, S., Li, L. Z. X., Li, Y., Huntingford, C., Ciais, P., et al. (2020). Summer soil drying exacerbated by earlier spring greening of northern vegetation. *Science Advances*, *6*(1), eaax0255. https://doi.org/10.1126/sciadv.aax0255

Niu, G.-Y., Yang, Z.-L., Dickinson, R. E., Gulden, L. E., & Su, H. (2007). Development of a simple groundwater model for use in climate models and evaluation with Gravity Recovery and Climate Experiment data. *Journal of Geophysical Research*, *112*(D7), D07103. https://doi.org/10.1029/2006JD007522